2022

Investigating Ground Interactions of a Rotocraft Landing Vehicle on Titan

Adam Rozman
University of Central Florida

INVESTIGATING GROUND INTERACTIONS OF A ROTORCRAFT LANDING VEHICLE ON TITAN

by

ADAM ROZMAN

A thesis submitted in partial fulfillment of the requirements
for the Honors in Major Program in Mechanical Engineering
in the College of Engineering and Computer Science
and in the Burnett Honors College
at the University of Central Florida
Orlando, Florida

Spring Term
2022

Thesis Chair: Dr. Michael Kinzel

ABSTRACT

The exploration of celestial bodies has recently advanced from rovers to rotorcraft. This includes the recent flights of Mars Ingenuity and the upcoming Dragonfly mission to explore the terrain of Saturn's moon Titan as part of NASA's New Frontiers Program [1]. Flight-based landers can travel quickly to sites kilometers apart and land in complex terrain [2]. Although cruise conditions for these rotorcrafts are well understood, studies are necessary to understand take-off and landing. In ground effect conditions, a rotor wake impinges and reflects off the ground, creating changes in aerodynamics such as increased lift. Additionally, operating over loose surfaces, the rotors can create clouds of dust obscuring the vehicle's sensors, a hazard termed "brownout" from rotorcraft landing in sandy and snowy conditions on Earth. Take-off and landing events involve interactions between the rotor wake, fuselage, and ground, and lead to a multi-phase interface between the fluid atmosphere and the dispersed dust particles [3]. The objective of this study is to computationally model and evaluate ground effect aerodynamic forces on the Dragonfly rotorcraft lander. A calculation of sediment distribution across the surface of the vehicle will provide insight to which components might be most affected by brownout.

TABLE OF CONTENTS

CHAPTER ONE - INTRODUCTION 1

CHAPTER TWO – MODEL DESIGN AND METHODOLOGY 4

CHAPTER THREE – GROUND EFFECT INVESTIGATION 7

CHAPTER FOUR – EULERIAN MULTIPHASE BROWNOUT MODEL 13

CHAPTER FIVE – DISCUSSION AND CONCLUSION 17

REFERENCES 19

LIST OF FIGURES

Figure 1: Geometry and force sign convention used in model 4

Figure 2: Computational mesh of vehicle surface (left) and cross-section of coaxial propeller refinement (right) 5

Figure 3: Grid Convergence Study of Aerodynamic Loads 6

Figure 4: Midplane velocity profiles at altitudes of 14, 11, 7, and 5 meters (left-to-right, top-to-bottom) 7

Figure 5: Dragonfly Near-Ground Aerodynamic Loads 8

Figure 6: Midplane velocity profiles at altitudes of 3, 2, 1, and 0 meters (left-to-right, top-to-bottom) 9

Figure 7: Streamlines of the Vehicle in Power on the Ground 10

Figure 8: Lift in Ground Effect 11

Figure 9: Body Drag in Ground Effect 11

Figure 10: Pitching Moment in Ground Effect 12

Figure 11: Unsteady Time Quadcopter Dust Cloud Formation 14

Figure 12: Quadcopter Body Surface Dust Distribution 15

Figure 13: Dispersed Multiphase Surface Volume Fraction Model 16

LIST OF TABLES

Table 1: Threshold Shear Values to Incite Dust Motion 14

LIST OF ABBREVIATIONS, ACRONYMS, AND NOMENCLATURE

CFD – Computational Fluid Dynamics

RANS – Reynolds-Averaged Navier-Stokes

BEM – Blade-Element Method

IGE – In Ground Effect

OGE – Out of Ground Effect

3D – Three Dimensional

CHAPTER ONE - INTRODUCTION

Computational Fluid Dynamics (CFD) programs use numerical methods to solve partial differential equations based on the Navier-Stokes equations, which define the conservation of mass, momentum, energy, and species in multiphase flow to determine the motion and interaction of fluids. Numerical models use algorithms to approximate solutions to these equations from user-defined boundary conditions like velocity or pressure at an inlet or stagnation (no-slip) at a wall. These calculations iterate until the solution stably approaches its asymptotic limit within a residual tolerance, whereupon the model is considered to have "converged."

A crucial component of simulating fluid flows is the modeling of turbulence. Turbulence occurs at high Reynolds numbers when inertial forces dominate viscous forces and produces highly irregular motion that facilitates mixing and energy dissipation. The Reynolds-Averaged Navier-Stokes (RANS) approach to solving turbulent flow modifies the Navier-Stokes equations by separating velocity, pressure, energy, and species ratio into mean and fluctuating components which are generated by one of the K-epsilon, K-Omega, or Spalart-Allmaras models [4]. RANS is relatively low in computational cost, and higher resolution can be achieved with more computationally expensive turbulence methods such as Detached Eddy Simulation, Large Eddy Simulation, or Direct Numerical Simulation [5].

The first step in investigating the Dragonfly vehicle's ground interaction is to model the flow created by the vehicle's eight rotors. CFD analysis of rotary wings (or propellers) can be divided into two main approaches: blade-resolved and blade-modeled. A blade-resolved model uses RANS or other methods to directly solve around the resolved geometry of the rotor,

requiring a very fine computational mesh that can take days to run on a supercomputer [6]. Blade-modeled approaches on the other hand, like the blade-element momentum theory and body force method, simulate the effect of rotors without resolving their geometries. These methods do not capture all the rotor behavior, such as wingtip vortices, but are exponentially cheaper in computational time. The Blade-Element Method (BEM) splits a cylindrical volume "virtual disk" into sections and introduces a momentum term into the equations of the mesh cells calculated from user-defined rotor blade characteristics [4].

Once the flow of the continuous phase (atmosphere) is modeled, the dispersed phase (dust) behavior can be calculated with either a Lagrangian or Eulerian approach. In a Eulerian approach, equations are solved for the system as a whole. The dispersed particles are influenced by the inertia of the continuous fluid represented with an added virtual mass equaling a constant multiplied by the mass of the continuous fluid displaced. Dispersed multiphase often uses one-way coupling by default, meaning that the continuous fluid affects the dispersed but the effects of the dispersed phase on the continuous are ignored. This method is accurate for small, dispersed phase volume fractions. The Lagrangian method instead tracks the path of particles through the medium. The dispersed phase is introduced from "injectors" which allow control over the size, velocity, and exact location where particles are added. Similar to the dispersed multiphase approach, this method assumes particles are spheres and is only valid when the volume fraction of particles is less than 10% [7].

A rotor operating close to the ground experiences a disturbance in flow as the slipstream is deflected by the ground, resulting in an increased thrust for a given power. This effect is noticeable at heights less than one diameter of the rotor, and has the most effect at heights less

than one-half diameter of the rotor [8]. A rotorcraft in this condition of increased thrust is known to be operating In Ground Effect (IGE), and Out of Ground Effect (OGE) at higher altitudes. Aerodynamic loads like lift, drag, and pitching moment are also affected IGE, but they vary greatly depending on the fuselage of the rotorcraft and cannot easily be predicted analytically.

Ground effect for rotorcraft has been studied for nearly a century, and a few predictive models have been developed such as the most well-known Cheeseman & Bennett model; however, it is accepted that models for ground effect in helicopters are not sufficient to apply to multirotors, and as such, some have attempted to formulate new models of ground effect [9]. This study will investigate the behavior of aerodynamic loads on the Dragonfly rotorcraft lander with proximity to the ground, as well as describe the multiphase behavior of clouds of dust created by the rotors operating IGE known as brownout. This hazard poses potential damage to the body and rotors of the vehicle, as well as obstruction of sensors critical to flight and landing.

CHAPTER TWO – MODEL DESIGN AND METHODOLOGY

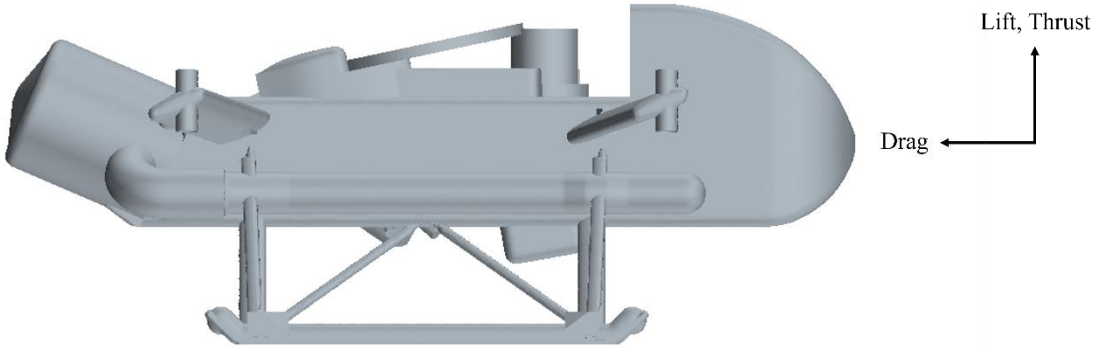

Figure 1: Geometry and force sign convention used in model

CFD simulations were run using Siemens Simcenter STAR-CCM+ Version 16.06.010 (double precision). The model included a Three-Dimensional (3D) simplified full-body geometry of the Dragonfly lander, disregarding minor protrusions including scientific instruments and antennas as seen above in Figure 1. All eight rotors of Dragonfly's coaxial rotors were modeled using BEM at a constant operating rotor speed. Ground effect analysis included calculations of the drag, body lift, pitching moment, and rotor thrust at various heights above a no-slip wall boundary. All cases were run using a static body parallel to the ground and a 0.5 m/s inlet velocity to the front of the vehicle. Additionally, Titan atmospheric conditions of 5.35 kg/m^3 density, 6.0E-6 Pa·s dynamic viscosity, and a gravitational constant of 1.352 m/s^2 were used.

The model assumed turbulent Reynolds conditions through the entire domain as well as constant density, or incompressible flow. Finally, the shear stress on the ground calculated using

BEM loses some accuracy as the approach does not capture the effect of high-shear wingtip vortices.

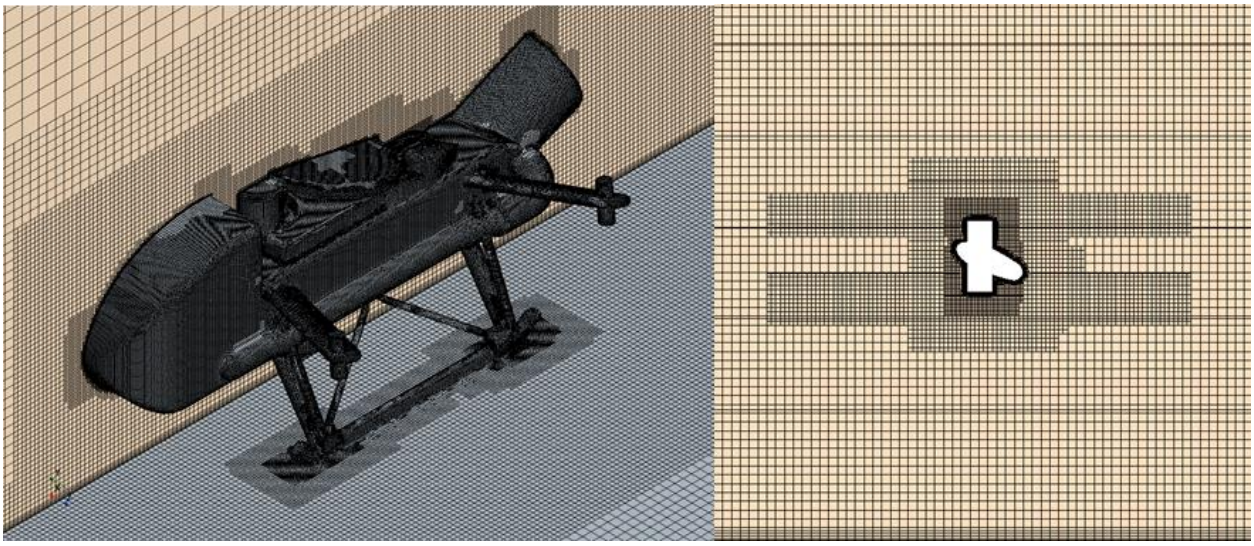

Figure 2: Computational mesh of vehicle surface (left) and cross-section of coaxial propeller refinement (right)

The computational model was built within a 30m x 30m x 30m cuboid region with a no-slip wall boundary for the ground and vehicle surface. The mesh was constructed with surface mesh refinement on the lander geometry, trimmed volumetric refinement surrounding the lander, as well as finer trimmed mesh over the rotor regions as seen above in Figure 2. A 2mm-thick prism layer was added to the vehicle surface to capture the boundary layer for accurate body forces.

A mesh convergence study for the model was conducted for aerodynamic loads using the methodology provided by Roache [10]. Three different mesh sizes were generated for the 14-meter altitude case with roughly 14, 10, and 6 million cells. Order of convergence was calculated using the extracted values, and the infinite mesh Richardson Extrapolate was determined. The

normalized convergence of lift, drag, pitching moment, and thrust can be seen plotted below in Figure 3.

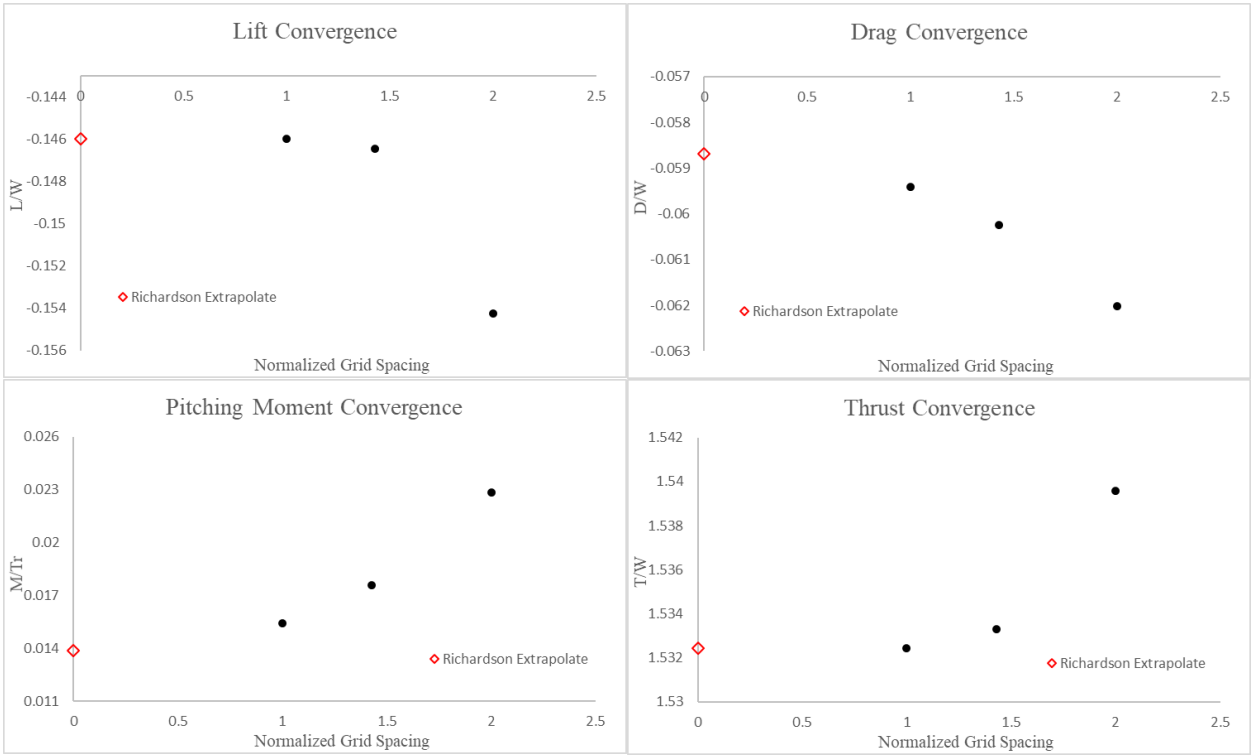

Figure 3: Grid Convergence Study of Aerodynamic Loads

CHAPTER THREE – GROUND EFFECT INVESTIGATION

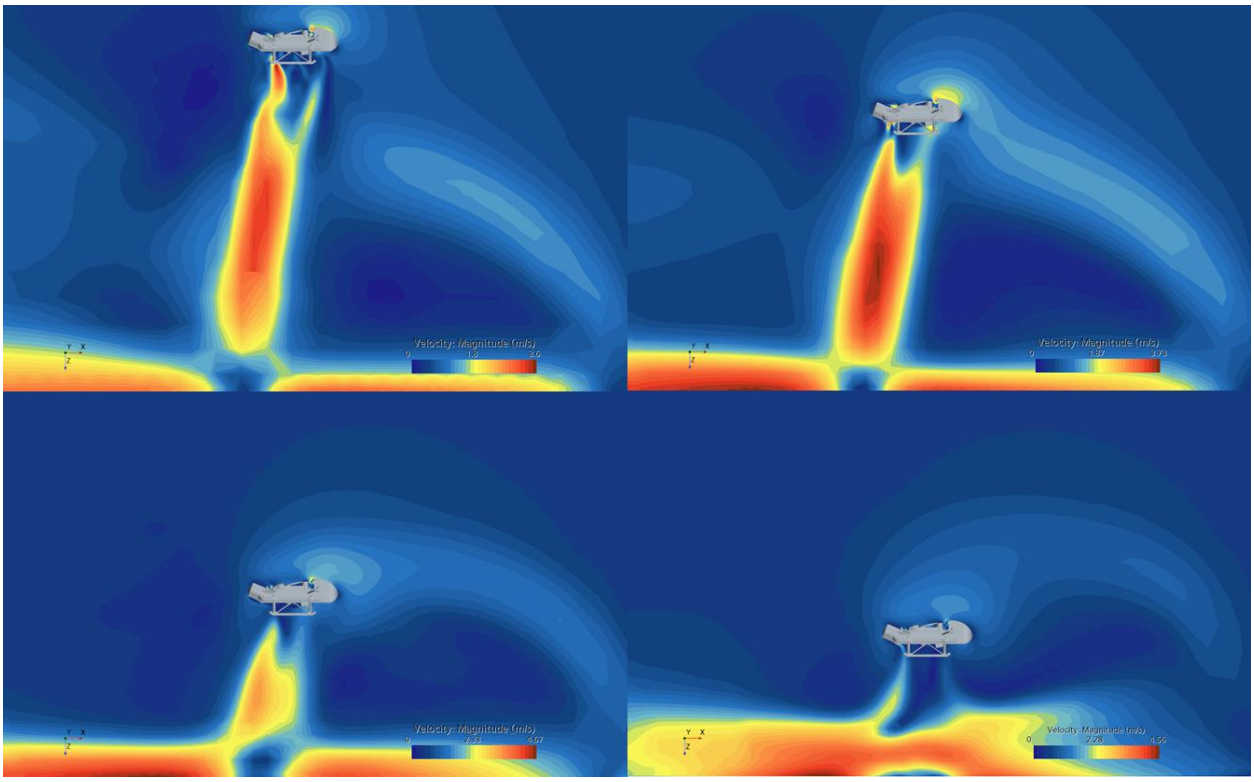

Figure 4: Midplane velocity profiles at altitudes of 14, 11, 7, and 5 meters (left-to-right, top-to-bottom)

Ground effect analysis included calculations of the drag, body lift, pitching moment, and rotor thrust at intervals of height descending from 14 meters above the ground boundary. Velocity profiles for the solutions to the first four cases can be seen above in Figure 4.

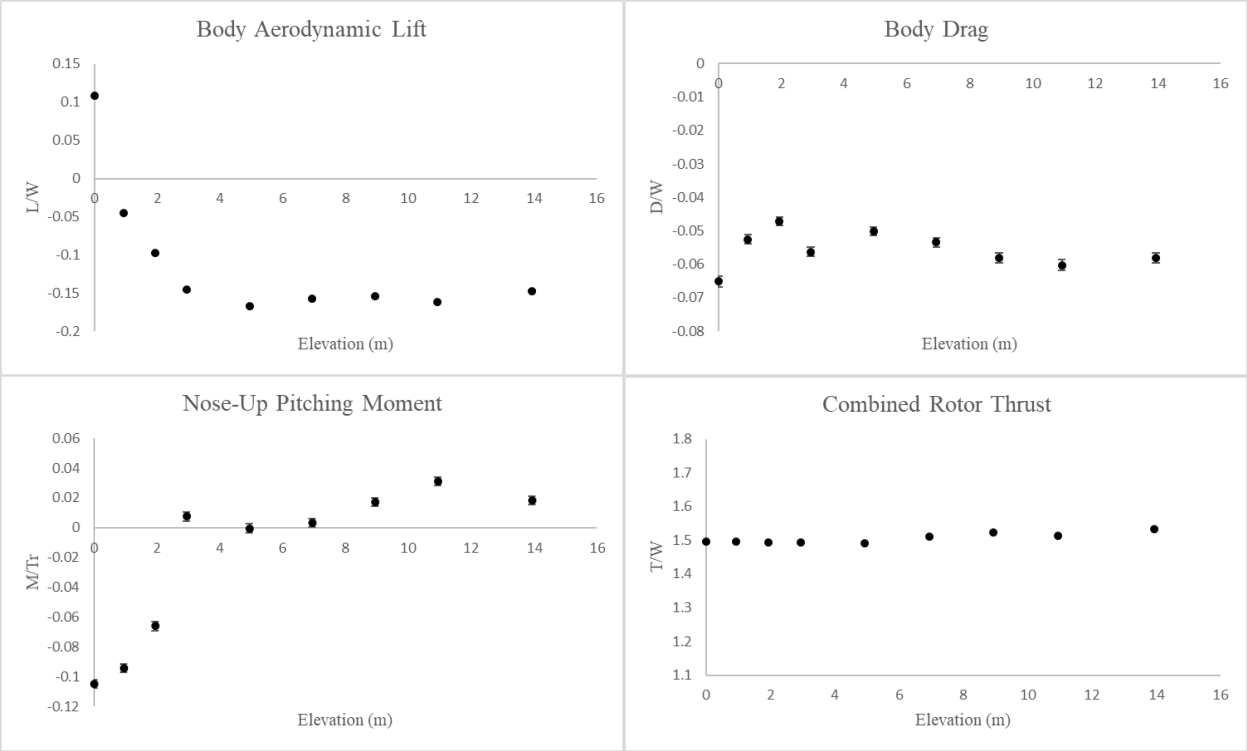

Figure 5: Dragonfly Near-Ground Aerodynamic Loads

Normalized aerodynamic loads are plotted above in Figure 5 against elevation from the bottom of the landing gear to the ground in meters. Lift, drag, and thrust forces are normalized by the weight of the vehicle, and pitch moment is normalized by the torque generated by one rotor revolving at normal speed.

In OGE hover away from the ground there is a significant negative aerodynamic lift, or download, and negative drag on the body. In a case of equivalent inlet velocity without propellers, lift is less than a tenth of this value and drag is negligible. Thus, it can be concluded that the download and negative drag are caused mainly by the interaction of the rotor downwash with the geometry of the arm fairings, visible in Figure 1, which have a positive angle of attack airfoil cross section to minimize drag during forward flight inclination. The nose-up pitching

moment appears to be created by a low-pressure region at the top of the vehicle behind the nose as visible in Figure 4. Thrust is not significantly affected by vehicle altitude within the range of altitudes for this study. This is not unexpected, as the height of the landing gear keeps the vehicle higher than 1.5 times the radius of the rotors, and literature suggests that the thrust increase from rotor ground effect is most prevalent within one rotor radius of the ground [8].

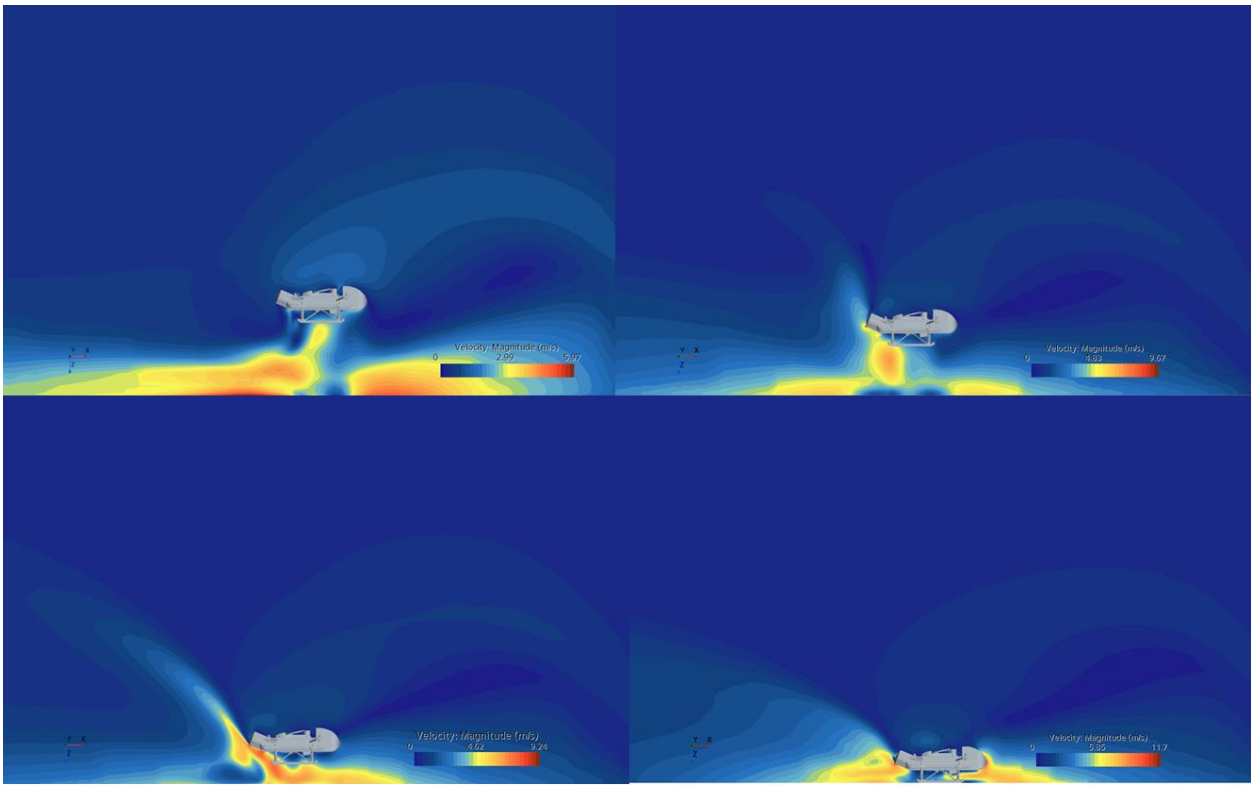

Figure 6: Midplane velocity profiles at altitudes of 3, 2, 1, and 0 meters (left-to-right, top-to-bottom)

Below an altitude of five meters, the download on the body decreases as the rotor downwash is deflected by the ground, trapped below the fuselage, then re-ingested by the aft rotors. This "fountain flow" between the underbody of the fuselage and ground generates upload with proximity to the ground has been documented experimentally for tiltrotors [11]. Lift is maximized with the vehicle skids touching the ground, where it overcomes the download created

by flow over the arms. This transition from induced download to upward lift under one meter from the ground can help descent stability, slowing and lessening the impact of landing.

As seen from the streamlines in Figure 7 below, air that is not re-ingested is forced toward the nose of the vehicle, creating a low-pressure area under the front of the fuselage which increases forward drag and induces a nose-down moment. The landing controller must consider increased drag at low altitude so as not to overshoot the desired landing site, and most significantly, the change from nose-up to nose-down pitching moment to maintain level flight and safe landing.

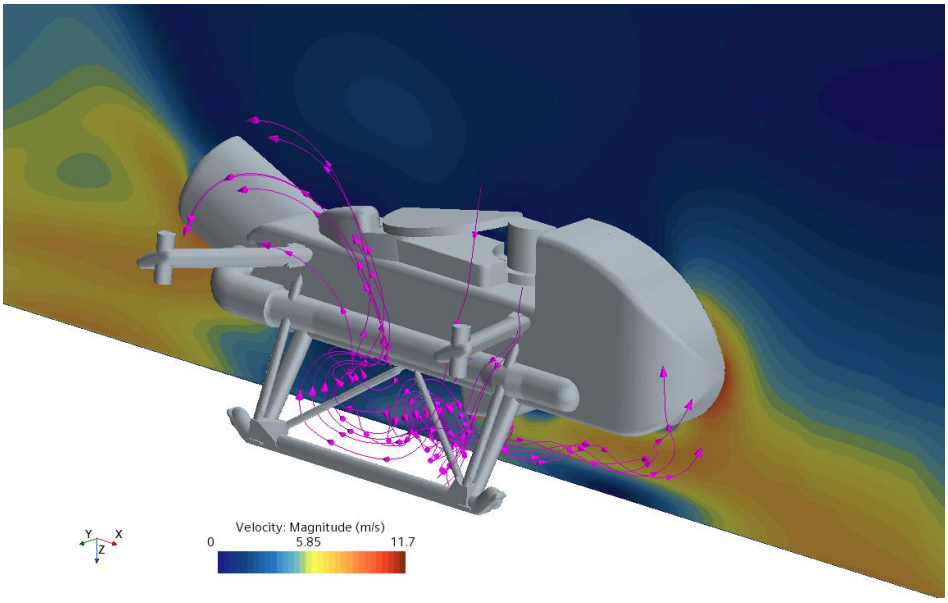

Figure 7: Streamlines of the Vehicle in Power on the Ground

Unusual values of pitch and drag occur at an altitude of three meters with a higher nose-up pitch and forward drag appearing than the trend would suggest. This appears to be caused by the recirculation vortex ahead of the fore rotors meeting the downwash of the rotors deflected by the ground, causing a secondary vortex of high pressure to form under the nose of the fuselage.

Below this altitude, a high-pressure region of flow reversal forms on the upper surface of the tail, causing a nose-down pitching moment. Nonetheless, the general trend in aerodynamic loads is evident.

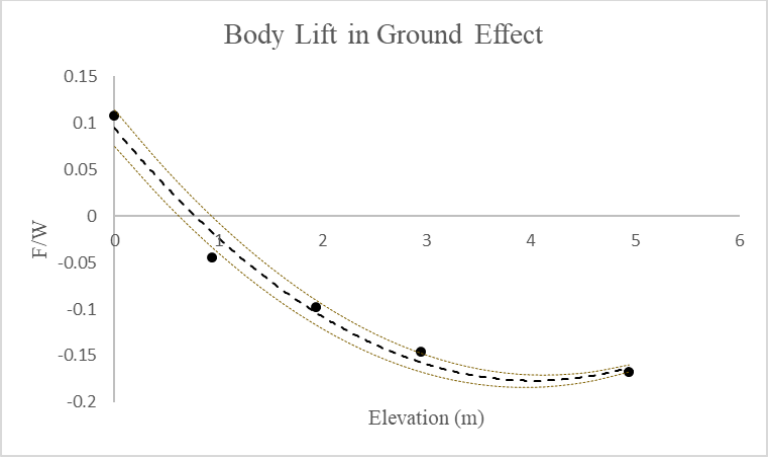

Figure 8: Lift in Ground Effect

Normalized body lift within ground effect as seen above in Figure 8 can be approximated by a second-order function of altitude below five meters

$$f(x) = 0.0167x^2 - 0.1347x + 0.0944, \quad x \leq 5 \tag{1}$$

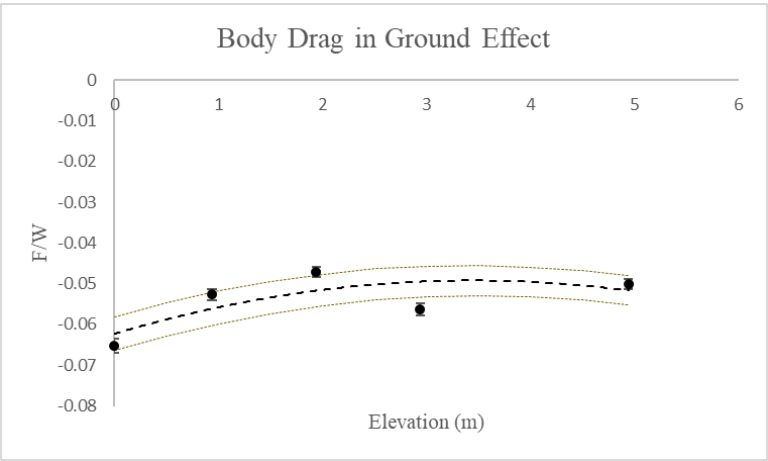

Figure 9: Body Drag in Ground Effect

Drag within ground effect as seen above in Figure 9 can be approximated by a second-order function of altitude below five meters

$$f(x) = -0.019x^2 - 0.1306x - 1.072, \quad x \leq 5 \tag{2}$$

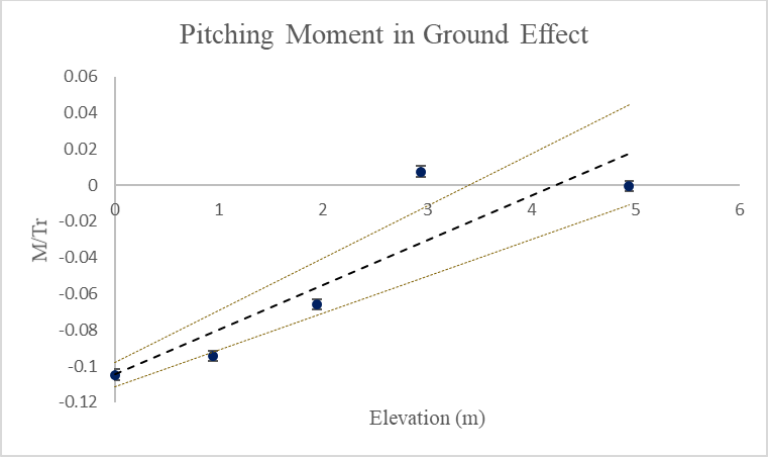

Figure 10: Pitching Moment in Ground Effect

Finally, pitching moment within ground effect as seen above in Figure 10 can be approximated by a linear function of altitude

$$f(x) = 0.0246x - 0.1047, \quad x \leq 5 \tag{3}$$

CHAPTER FOUR – EULERIAN MULTIPHASE BROWNOUT MODEL

An examination of brownout conditions called for the assessment of an Eulerian two-phase method of modeling air and perturbed dust. Existing brownout models often use a form of Lagrangian particle tracking and assume a one-way fluid coupling [3] where the carrier fluid affects the dispersed particle but not the inverse. The Eulerian approach allows the interaction between BEM-modeled propellers and dust to be captured, in contrast to a Lagrangian or Dispersed Multiphase Eulerian model, in which the flow solver is frozen before introducing dust. An Eulerian approach is also less computationally expensive.

Dust entry can be defined on the ground surface by calculating the wall shear stress to excite dust of a given diameter using the shields parameter calculation for initiation of sediment motion. The equation

$$\theta_c = \frac{\tau}{(\rho_s - \rho)gD} \tag{4}$$

was used where ρ represents the density of the fluid, ρ_s the density of the sediment, g the gravitational acceleration, D the particle diameter, and θ_c the critical shields parameter which can be assumed to be $\theta_c = 0.045$ for a high shear Reynolds number [12]. For example, the shear stress threshold to incite motion in a variety of particle diameters can be seen below in Table 1.

Table 1: Threshold Shear Values to Incite Dust Motion

Particle Diameter (micron)	Earth Threshold Shear Stress (Pa)	Titan Threshold Shear Stress (Pa)
5	0.005957	0.000991
10	0.011914	0.001983
20	0.023827	0.003965
50	0.059569	0.009913
100	0.119137	0.019826
300	0.357412	0.059477
500	0.595687	0.09913
1000	1.191374	0.198255

It is evident that dust motion begins at shear stress values an order of magnitude lower on Titan than on Earth, influenced by the combined higher density of air and lower gravitational force.

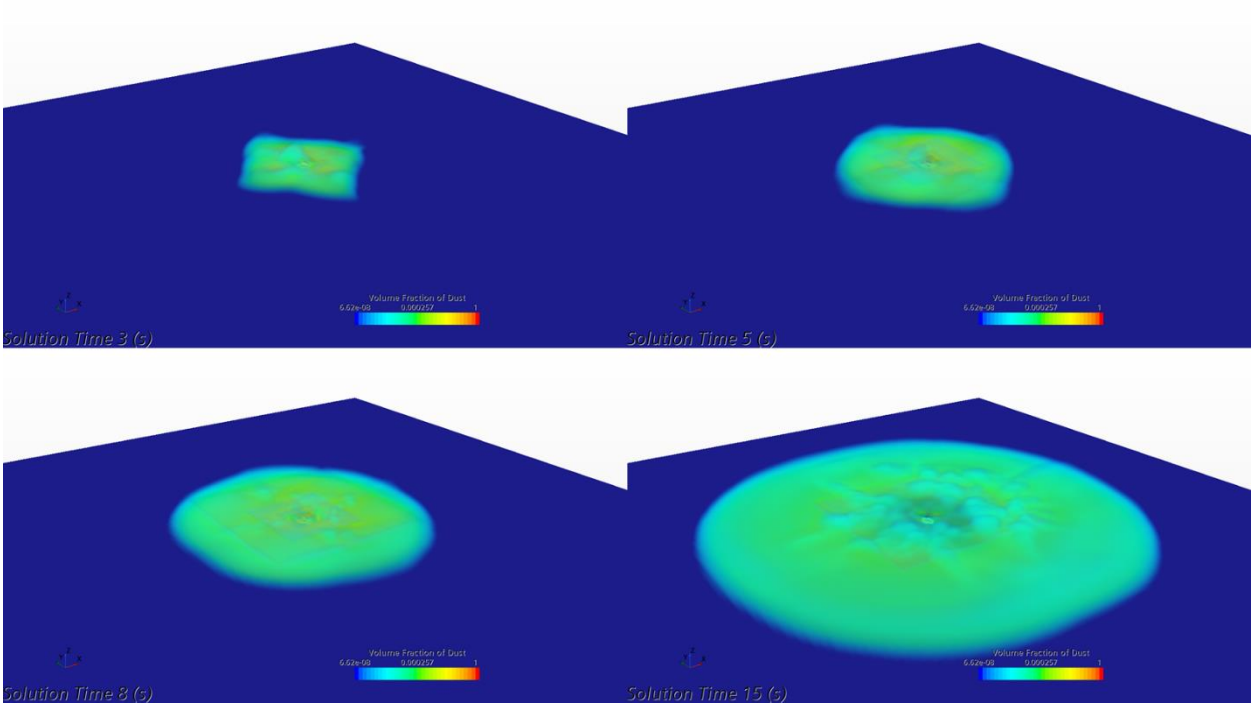

Figure 11: Unsteady Time Quadcopter Dust Cloud Formation

The Eulerian brownout simulation method was developed using a model of a DJI F450 quadcopter at a height of one rotor diameter from the ground, with four rotors modeled using

BEM at constant rotation speed. The simulation was first run with a single-phase fluid domain of air to calculate shear stress on the ground. Next, the floor boundary was set to an inlet with a dust-to-air volume fraction equal to one where shear stress exceeded the threshold motion shear as described above, and zero elsewhere. The dust cloud formed using an unsteady-time model over fifteen seconds can be seen above in Figure 11. A steady-time model option was also simulated to view the average volume fraction of dust across the drone surface. The results of this steady model can be seen below in Figure 12. The magnitude of the volume fraction is not particularly relevant, but it is useful to view the relative distribution of dust across the drone body. It is evident that the highest amount of dust impacts the middle to outward end of the arms of the drone, as well as a lower concentration of dust impacting the central plate of the body.

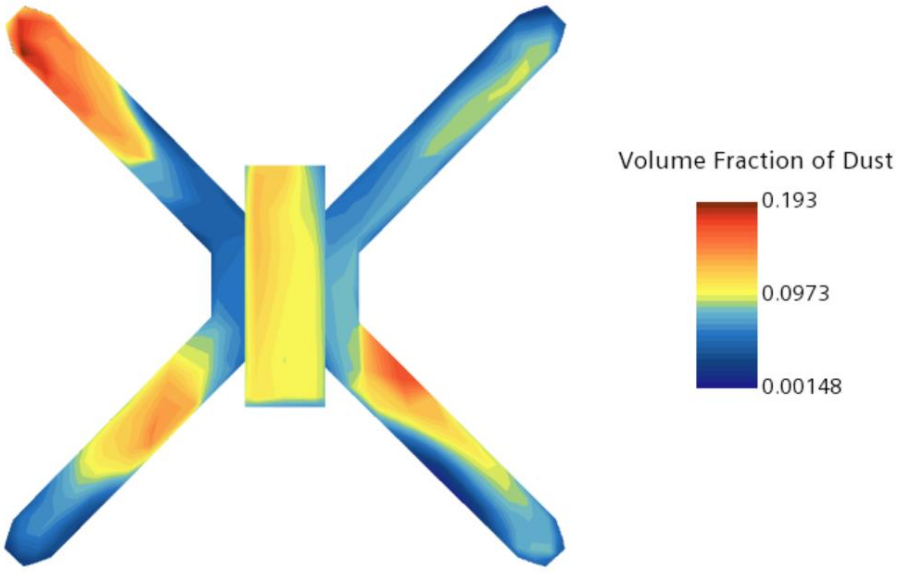

Figure 12: Quadcopter Body Surface Dust Distribution

The Eulerian two-phase modeling approach was subsequently applied to the Dragonfly model at identical operating conditions used for the aerodynamic loads study. However, the

approach did not yield stable, meaningful results. Therefore, a Eulerian Dispersed Multiphase solver was applied to the model instead, which can be used to capture the volume fraction of dust across the surface of the vehicle. This model cannot be used in tandem with the BEM model for the propellers, so the flow field of air must be "frozen," or set not to update. The results of the Eulerian Dispersed Multiphase model can be seen below in Figure 13. Most of the dust impacts the top of the vehicle, most notably toward the rear of the circular antenna and the cylindrical generator at the tail, and the arms of the vehicle. Dust also spreads across the bottom surface of the drone with most of the dust towards the rear. The distribution along the bottom is much less uniform due to the high instability of the recirculation in the high-pressure area below the vehicle.

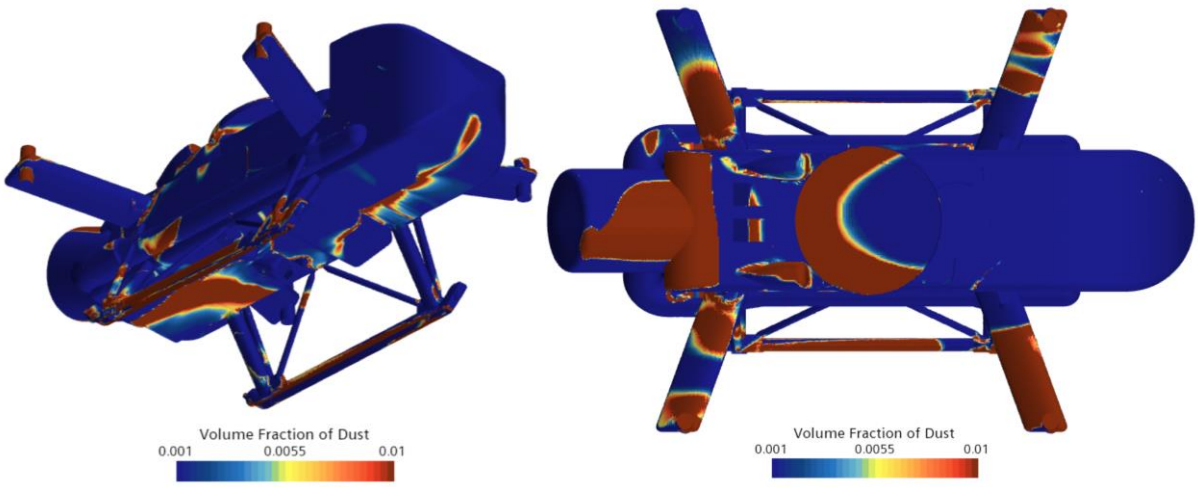

Figure 13: Dispersed Multiphase Surface Volume Fraction Model

CHAPTER FIVE – DISCUSSION AND CONCLUSION

Calculating the aerodynamic loads on the Dragonfly vehicle within proximity to the ground using CFD proved to be a valuable undertaking. This investigation supports the findings of established literature regarding the development of an upload on the body near the ground due to recirculation vortices forming below the fuselage. Additionally, the study did not show a noticeable increase in thrust near the ground, which is acceptable since the landing gear keeps the vehicle just out of the proximity from the ground at which a significant increase in thrust would occur. A further investigation of thrust produced by a set of coaxial rotors within close proximity (less than one-half rotor diameter) to the ground would be beneficial to elucidate the ground effect behavior of such a multirotor vehicle. Additionally, evaluating aerodynamic loads with the vehicle at different angles to the ground as well as different rotor speeds would provide valuable data.

The behavior of drag and pitching moment with proximity to the ground for the Dragonfly vehicle is novel, as these forces are hard to predict and greatly depend on the geometry of the vehicle. Most notably, the pitching moment changes signs from a nose-up to a nose-down moment below an altitude of five meters, which could pose issues for the landing controller if not accounted for. The increase in negative drag at these altitudes should also be considered in the controller so as not to overshoot the desired landing area.

The brownout model posed to be the most difficult aspect of the investigation. Predicting dust kickup using the shields parameter served as a useful guideline, and the Eulerian two-phase modeling approach provides a quick simulation of dust cloud created. However, this approach

does not permit dust to settle back to the ground; this was compensated for by increasing the computational region to preserve an infinitesimal volume fraction at the boundaries. This prevents a converging steady solution and adds computational cost as more mesh is required. This modeling technique still has value for simulating dust cloud formation, but more work must be done to get the two-phase approach as stable as a Dispersed Multiphase model. Such a model would be able to capture surface volume fraction of dust as well as the cloud formed.

Also, the simulation is limited by some of the computational assumptions made. A drawback of BEM propeller modeling is that propeller wingtip vortices, which are high in shear, are not properly resolved. Therefore, a blade-resolved model might be desired eventually to better represent shear stress.

Part of the scope of this project was to compare a computational brownout model of a quadcopter to experimental data. Going forward, it is desired to design an experiment to capture the ground shear stress distribution of the DJI F450 drone as well as the spread of dust impacting the surface of the drone. This would provide validation for the computational data and allow them to be more readily applied to the Dragonfly project where experimentation will not be possible until the vehicle is on Titan.

REFERENCES

1. John Hopkins University Applied Physics Laboratory, “Dragonfly,” 2021, https://dragonfly.jhuapl.edu

2. Lorenz, R. D., Schmitz, S., Kinzel, M., “Prediction of aerodynamically-triggered condensation: Application to the Dragonfly rotorcraft in Titan’s atmosphere,” Aerospace Science and Technology, Vol. 114, 2021.

3. Govindarajan, B. M., Leishman, J. G., “Predictions of Rotor and Rotor/Airframe Configurational Effects on Brownout Dust Clouds,” AIAA Journal of Aircraft, Vol. 53, No. 2, 2016.

4. Siemens, “User Guide: STAR-CCM+ Version 16.06,” 2021.

5. Thai, A., Grace, S., Jain, R., “Effect of Turbulence Modeling Selection Within Helios for Small Quadrotor Aerodynamics,” AIAA Journal of Aircraft, pp. 1-19, 2022.

6. Cornelius, J., “Efficient CFD Approaches for Coaxial Rotor Simulations,” Master’s Thesis, Dept. of Aerospace Engineering, Pennsylvania State University, 2019.

7. Persson, T., “Eulerian-Lagrangian Modeling of Multicomponent Spray for Aseptic Treatment of Carton Bottles in the Food Process and Packaging Industry,” Master’s Thesis, Dept. of Applied Mechanics, Chalmers University of Technology, 2013.

8. Leishman, J. G., “Principles of Helicopter Aerodynamics,” Cambridge, Cambridge University Press, 2000, pp 185-189.

9. He X, Leang K. K., “A new quasi-steady in-ground effect model for rotorcraft unmanned aerial vehicles,” ASME, dynamic systems and control conference, Vol. 3, Park City, UT, USA, Oct. 2019

10. Slater, J., “Examining Spatial (Grid) Convergence”, National Program for Applications-Oriented Research in CFD, 2021. https://www.grc.nasa.gov/www/wind/valid/tutorial/spatconv.html

11. Matus-Vargas, A., Rodriguez-Gomez, G., Martinez-Carranza, J., “Ground Effect on Rotorcraft Unmanned Aerial Vehicles: a Review,” Intelligent Service Robotics, Vol 14, No. 1, 2021.

12. Zhixian, C., Gareth, P., Jian, M., “Explicit Formulation of the Shields Diagram for Incipient Motion of Sediment,”